Frontiers in Computing and Intelligent Systems
ISSN: 2832-6024 | Vol. 2, No. 2, 2022

Closed Trajectory Optimization for Aerial Base Station: An Energy Efficiency Design

Fengyuan Tian

Department of Engineering, King's College London, London, WC2R 2LS, United Kingdom

Abstract: By optimizing the energy-efficient flight trajectory of unmanned aerial vehicles (UAVs), UAV-based aerial base stations (BSs) can provide longer communication services to more ground nodes (GNs) under the UAV battery limitation. Path discretization method and successive convex approximation (SCA) algorithm have been shown to be effective techniques in the design of the energy-aware UAV one-way trajectory along a few GNs. Compared with current studies, this paper designed and compared different optimal closed UAV trajectories among multiple GNs under a wide range of changing communication requirements. Meanwhile, a more complex and realistic scenario is considered where the UAV visits the ground nodes sequentially without repetition from a centrally located terrestrial base station and returns to the starting point in the end. To thoroughly analyze this problem, two UAV trajectory designs are proposed in this paper. One is to use the fly-hover-communicate protocol as a benchmark for comparison, and the other is to require that the UAV should fly and communicate with ground nodes simultaneously, named the fly-over scheme. The simulation results show that, in general, the proposed fly-over scheme outperforms the benchmark results, while in the case of high and low communication demands, the energy-saving performance of both is very similar. Therefore, advice can be given on the design of the UAV trajectory depending on different situations.

Keywords: UAV communication; Aerial base stations; Trajectory optimization.

1. Introduction

With the emerging applications of the forthcoming beyond fifth-generation (B5G) and sixth-generation (6G) net- works, the explosion of mobile traffic results in higher requirements of existing equipment for handling the numerous connectivity demands with not even low latency but also high speed. Additionally, the further investment and operational costs to address this problem will be a significant burden to telecommunication operators. In current studies, unmanned aerial vehicles (UAVs) are expected to demonstrate instrumental abilities for public safety and disaster management under the heterogeneous network (HetNet) structure [1]- [3]. Due to its inherent high mobility and the favorable line-of-sight (LoS) communication circumstances, the UAV can efficiently support areas with high connectivity demands or system overload in wireless communication systems [4]- [6]. In particular, the UAV-based enhanced mobile broadband (eMBB) is identified as a great success in wireless cellular networks [7].

Early research focused on the hovering altitude and signal coverage of static flying base stations (FBSs) [8]- [10], while recent study emphasis has moved to the dynamic UAV communication systems to thoroughly utilize the flexibility of drones. Therefore, by exploiting the mobility of UAVs, UAV trajectory design is significant but challenging in studying this system, as it commonly requires trade-offs among energy consumption, communication throughput, and delay [11]. Some studies in [12]- [15] optimized the UAV flight trajectory for maximizing the transmission rate. Wonseok Lee et al. [16] optimized the UAV trajectory to obtain the optimal deployment where mobile ground users were considered.

In more practical scenarios, the energy consumption of drones is quite vital for trajectory design because the amount of power that can support the flight of a UAV completing its mission is limited. To address this, studies in [17]- [19] proposed the energy-efficient UAV trajectory for a single UAV flying over a single node under the maximum flying speed and completion time constraints. On this basis, Zeng et al. [20] extended the work by forming a traveling salesman prob- lem (TSP) where the UAV should visit three ground nodes (GNs) sequentially without repetition instead of a single node. They proposed a one-way trajectory with the minimum energy consumption for the rotary-wing UAV by introducing the path discretization method and successive convex approximation (SCA) algorithm. Their results showed that it was more energy efficient to communicate while the UAV was in flight than to hover for communication after flying to the corre- sponding position.

However, this work in [20] and other relevant studies [21] provided a one-way trajectory along only three GNs. To explore a more general and complex scenario, Shavbo Salehi et al. considered more GNs but still a one-way trajectory in the case that the UAV flew and hovered above each node [22], [23]. Tingting Lan et al. [24] obtained the one-way energy-efficiency trajectory among a large number of GNs under certain communication demands but they have not analyzed the effect of the changing communication throughput requirements on the trajectory design. Additionally, authors in [25] designed a closed flying trajectory with multiple GNs, but they focused on the maximum number of ground users served under the UAV battery limitation. Nevertheless, the closed UAV trajectory optimization with the total energy consumption minimization among multiple GNs under variant transmission demands is a further valuable direction to explore for the UAV communication system design, which has not been discussed in detail. Therefore, the energy consumption in this paper is minimized under the scenario where the UAV-based FBS departs from a ground base station that provides power charging, visits more GNs only once, and returns to the departure point. This forms a closed flight trajectory, and this work first obtains the optimal fly-hover-communicate trajectory as the benchmark. Next, the UAV is considered to fly over the GNs instead of hovering while

communicating with the GNs, which is a general scenario named the fly-over scheme. In addition, this paper compares the performance of these two methods under a wider range of various communication requirements. The results show that the fly-over scheme did not outperform the fly-hover protocol under extremely high or low communication demands.

Based on the baseline scenario and system model designed, this work has formulated the energy minimization problem with several constraints. The goal is to obtain minimal energy consumption under the optimal communication allocation time, the UAV trajectory, and the total completion time. This problem is non-convex which is hard to solve efficiently. The basic idea is to convert a non-convex optimization problem into a convex optimization problem by introducing the slack variable, applying genetic algorithm (GA) and SCA algorithms, as well as using the path discretization technique. The detail of the solution is introduced in Section 3.

2. System Model and Problem Formulation

2.1. System Model

In the basic scenario, an FBS-equipped drone departs from a ground base and visits different user nodes on the ground in turn, and each user node traverses only once and finally returns to the ground base. This paper objects to obtaining the flight trajectory that consumes the least energy. From Fig. 1, the hypothetical square map with length L. The ground base station is assumed to be located at the map's center with coordinates [$\frac{L}{2}$, $\frac{L}{2}$]. Also, this work currently considers a set of N user nodes randomly distributed on the map with their coordinates [xn, yn] (n ∈ [1, N]), which are denoted by wn . In this system, the work assumes the flying altitude H is fixed and the total completion time of the whole flight is Tt . The trajectory of the rotary-wing UAV is denoted as q(t) with 0 < t < Tt, which is a two-dimensional vector representing the position of the UAV (q(t) ∈ [x(t), y(t)]). Accordingly, the speed of the UAV v(t) is the derivative of q(t) under the maximum flying speed constraint Vmax . At time t ∈ [0, Tt], the distance between the UAV and GN n is calculated as dn(t) =^H2 + // q(t) − wn // 2 .

2.1.1. Communication model

For simplicity, the air-to-ground (AtG) links are considered to be mainly LoS links, and the None-line-of-sight (NLoS)

channels in the designed system are ignored. This is because the ability to use LoS links more effectively is one of the main reasons for deploying the FBS. Correspondingly, let hn(t) denote the path-varying channel for n − th GN at time t, which is given

$$h_n(t) = \frac{\beta_0 |g_n(t)|^2}{d_n(t)^{\tilde{\alpha}}}, \quad (1)$$

where β0 is the channel power when the distance between senders and receivers is d0 = 1m and $\tilde{\alpha}$ means the path loss exponent. The variable gn(t) is the channel coefficient representing the shadowing and the small-scale fading effect for

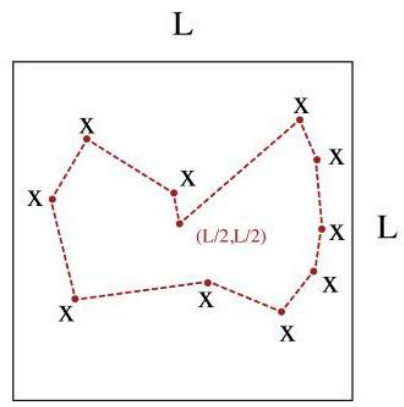

Figure 1. System Model Map

the n-th GN at time t. Correspondingly, it is shown that E [|gn(t)|2] = 1 [20]. Accordingly, the achievable transmission rate in bits per second (bps) for the UAV communicating to GN n at time t can be expressed as

$$R_n(t) = B \log_2 \left(1 + \frac{P h_n(t)}{\sigma^2 \Gamma}\right), \quad (2)$$

where B is the channel bandwidth, γ > 1 represents the gap between actual and ideal channel capacity. P denotes the transmission power of the UAV, and σ 2 is the noise power.

Then a binary variable is considered as λn(t), which indicates whether the ground node n is scheduled at time t. This paper applies the time-division multiple access (TDMA) protocol. It requires that the UAV can only communicate to zero and one GN at one time, and the relevant inequality is written as

$$\sum_{n=1} \lambda_n(t) \le 1, \forall t \in [0, T_t], \quad (3)$$

Then, the function of the aggregated expected throughput for node n is

$$\tilde{R}_n(T_t, \{q(t)\}, \{\lambda_n(t)\}) = \int_0^{T_t} \lambda_n(t) R_n(t) dt. \quad (4)$$

However, hn(t) varies with time, and the aggregated expected throughput is hard to calculate while the expected throughput n can be used to replace n. It can be given by

$$\begin{aligned} \bar{R}_n &= \int_0^{T_t} \lambda_n(t) B E\left[\log_2\left(1 + \frac{P h_n(t)}{\sigma^2 \Gamma}\right)\right] dt, \\ &\approx \int_0^{T_t} \lambda_n(t) B \log_2\left(1 + \frac{P E[h_n(t)]}{\sigma^2 \Gamma}\right) dt \\ &= \int_0^{T_t} \lambda_n(t) B \log_2\left(1 + \frac{\gamma_0}{\left(H^2 + \|q(t) - w_n\|^2\right)^{\alpha/2}}\right) dt, \end{aligned} \quad (5)$$

where γ0 is the signal-to-noise ratio (SNR) rate which is equal to, and α is the expected path loss exponent where α = $\tilde{\alpha}$.

2.1.2. Energy consumption model

The energy consumption of the rotary-wing UAV as the objective function can be divided into propulsion energy consumption and communication energy consumption.

The propulsion power consumption [19] is

$$P_T = P_0\left(1 + \frac{3V^2}{U_{tip}^2}\right) + P_i\left(\sqrt{1 + \frac{V^4}{4v_0^4}} - \frac{V^2}{2v_0^2}\right)^{1/2} + \frac{1}{2} d_0 \rho s A V^3, \quad (6)$$

where P0 is the blade profile power and Pi is the hovering induced power. v0 is the mean rotor-induced velocity when the UAV is hovering, Utip is the tip speed of the rotor blade, d0 is the fuselage drag ratio, and ρ presents the air density. s is the rotor solidity, and A presents the rotor disc area. Then, the communication power consumption is given as a fixed constant Pc. Additionally, when the UAV is hovering, the propulsion power consumption of hovering status can be obtained when

the UAV speed is equal to zero in (6), which is Phover = P0 + Pi.

To be more specific, P0 and Pi can be expressed as

$$P_0 = \frac{\delta}{8}\rho s A \Omega^3 R^3, \quad (7)$$

$$P_i = (1+\kappa)\frac{W^{3/2}}{\sqrt{2\rho A}}, \quad (8)$$

where δ is profile drag coefficient, Ω is the blade angular velocity, and R is rotor radius in P0 . Furthermore, in Pi, and κ is incremental correction factor to induced power while W is the aircraft weight.

Therefore, the total energy consumption is denoted as E (Tt , {q(t), {λn(t)), which is

$$E(T_t, \{q(t)\}, \{\lambda_n(t)\}) = \int_0^{T_t} P_T(v(t))dt + P_c \int_0^{T_t} \left(\sum_{n=1}^{N} \lambda_n(t)\right) dt. \quad (9)$$

Then, the optimization problem is formulated based on the rotary-wing UAV energy consumption model, subjecting to the required communication throughput and maximum flying speed limit.

2.2. Problem Formulation

The UAV trajectory optimization problem (P 1) based on the designed system model is formed as

$$P1: \min_{\{T_t, q(t), \lambda_n(t)\}} E(T_t, \{q(t)\}, \{\lambda_n(t)\}) \quad (10)$$

s.t.

$$\|q(t)\| \le V_{max}, At \in [0, T_t], \quad (10a)$$

$$R_n(T_t, \{q(t), \lambda_n(t)\}) \ge Q_n, An, \quad (10b)$$

$$q(0) = q_0, q(T_t) = q_0, \quad (10c)$$

$$0 \le q(t) \cdot x \le L, \quad (10d)$$

$$0 \le q(t) \cdot y \le L, \quad (10e)$$

$$\lambda_n(t) \in [0, 1], An \in N, At \in [0, T_t], \quad (10f)$$

$$\sum_{n=1}^{N} \lambda_n(t) \le 1, At \in [0, T_t], \quad (10g)$$

where Vmax is the maximum UAV speed, and Qn is a given expected required communication throughput for GN n. Furthermore, constraint (5c) indicates the closed UAV trajectory, and the q0 is the starting point for the departure of the UAV. The UAV is also required to fly within the range of the virtual map shown in constraints (10d) and (10e).

To handle this non-convex continuous optimization problem, this work applies two different UAV-to-ground communication schemes from the one-way trajectory design to the proposed system model with a closed trajectory. The first one is the fly-hover-communicate protocol as the benchmark for comparison. This means the UAV continuously visits the same number of hover locations as GNs, communicating with a corresponding GN at each location as it hovers. In this way, the problem can reduce to a more straightforward problem with finite variables by jointly optimizing the visiting order and hover locations. The other more general scheme considers the UAV communicating simultaneously while in flight. This paper introduces the path discretization method and SCA algorithm to solve this problem.

3. Solutions to the Problem

3.1. Solution under fly-hover-communicate protocol

Considering the UAV starts to provide service to GN n when hovering on one location, the problem (P 1) reduces to optimize the UAV visit order among N GNs, and the UAV flying speed among these hover locations. The q˜n ∈ R2 is denoted as the UAV hovering location for communicating to GN n. Therefore, for each GN n, the total communication time under the throughput requirement can be expressed as

$$T_n(\tilde{q}_n) = \frac{Q_n}{B \log_2\left(1 + \frac{\gamma_0}{(H^2 + \|\tilde{q}_n - w_n\|^2)^{\alpha}}\right)}. \quad (11)$$

Accordingly, the function of the total required hovering and communication energy for GN n can be formulated as follow

$$E_{hc} = (P_h + P_c)\sum_{n=1}^{N} T_n(\tilde{q}_n) = (P_h + P_c)\sum_{n=1}^{N} \frac{Q_n}{B \log_2\left(1 + \frac{\gamma_0}{(H^2 + \|\tilde{q}_n - w_n\|^2)^{\alpha}}\right)}, \quad (12)$$

where Ph = P0 + Pi and Pc denote the hovering power and communication power of the UAV, respectively.

For the propulsion energy consumption of the UAV, it is related to the total UAV flying distance Dtr after visiting all hover locations q˜n with the speed V (t). Referring to [20], the optimal flying speed of the UAV under the hover trajectory design needs to keep at the MR speed Vmr . Accordingly, the MR speed is the speed that minimizes the consumed energy per unit of flying distance. For the formulated problem, the UAV energy consumption per unit of flying distance can be defined as

$$E_0(V) = \frac{P(V)}{V} = P_0\left(\frac{1}{V} + \frac{3V}{U^2}\right) + P_i\left(V^{-4} + \frac{1}{4v^2}\right)^{1/2} + \frac{1}{2}d_0 \rho s A V^2. \quad (13)$$

Therefore, the MR speed can be obtained as Vmr = arg minV ≥0E0(V), and the UAV energy consumption per unit flying distance with MR speed is E0 = E0 (Vmr).

Furthermore, the total flying distance Dtr is determined by the sequence of accessing each GN. This work defines a variable Ω(n) ∈ {1, . . . , N to denote the index of hover location where the UAV is serving to GN n. Then, the function of Dtr is given by

$$D_{tr}(\{\tilde{q}_n\}, \{\Omega(n)\}) = \sum_{n=1}^{N-1} \|\tilde{q}_{\Omega(n+1)} - \tilde{q}_{\Omega(n)}\| + \|\tilde{q}_{\Omega(1)} - q_0\| + \|\tilde{q}_{\Omega(N)} - q_0\|, \quad (14)$$

where the second term and third term denote the distance of the first hover location and the last hover location from the starting point.

Therefore, the total UAV propulsion energy consumption can be given by

$$E_{tr}(\{\tilde{q}_n\}, \{\Omega(n)\}) = E_0^s D_{tr}(\{\tilde{q}_n\}, \{\Omega(n)\}). \quad (15)$$

Then, the total UAV energy consumption is shown as follow

$$E_{tot}(\{\tilde{q}_n\}, \{\Omega(n)\}) = E_{hc}(\{\tilde{q}_n\}) + E_{tr}(\{\tilde{q}_n\}, \{\Omega(n)\}). \quad (16)$$

Above all, the problem (P 1) can be transferred to (P2) as

$$P2: \min_{\{\tilde{q}_n\}, \Omega(n)} E \cdot D_{tr}(\{\tilde{q}_n\}, \{\Omega(n)\}) + \sum_{n=1}^{N} \frac{(P_h + P_c) Q_n}{B \log_2\left(1 + \frac{\gamma_0}{(H^2 + \|\tilde{q}_n - w_n\|^2)^{\alpha}}\right)}, \quad (17)$$

s.t.

$$[\Omega(1), \ldots, \Omega(N)] \in P, \quad (17a)$$

$$0 \le \tilde{q}_n \cdot x \le L, n = \{1, \ldots, N\}, \quad (17b)$$

$$0 \le \tilde{q}_n \cdot y \le L, n = \{1, \ldots, N\}, \quad (17c)$$

where P means the N ! possible combinations of permutations for N GNs. Problem (P2) is also hard to solve as it is a non-convex optimization problem. To solve it, this work first solves the TSP with the shortest flight distance by applying the GA when fixing the hover location. After obtaining the optimal visit order $\hat{\Omega}*$ (n), the work then reformulates the optimization problem to optimize the UAV hover locations. In the new problem, this study introduces the slack variables

Dtot and ηn = log2 (1 + $\left(H^2 + \|\tilde{q}_n - w_n\|^2\right)^{\alpha}$) and adds new corresponding constraints. Therefore, the new problem (P2.1)

can be given by

$$P2.1: \min_{\{\tilde{q}_n, D_t, \eta_n\}} E_0^* D_{tot} + \sum_{n=1}^{N} \frac{(P_h + P_c) Q_n}{B\eta_n} \quad (18)$$

$$s.t. \sum_{n=1}^{N-1} \|\tilde{q}_{n+1} - \tilde{q}_n\|^2 + \|\tilde{q}_1 - \tilde{q}_0\|^2 + \|\tilde{q}_N - \tilde{q}_0\|^2 \le D_{tot}, \quad (18a)$$

$$\eta_n \ge 0, \quad (18b)$$

$$0 \le \tilde{q}_n \cdot x \le L, n = \{1, \ldots, N\}, \quad (18c)$$

$$0 \le \tilde{q}_n \cdot y \le L, n = \{1, \ldots, N\}, \quad (18d)$$

$$\log_2\left(1 + \frac{\gamma_0}{\left(H^2 + \|\tilde{q}_n - w_n\|^2\right)^{\alpha}}\right) \ge A_n, \quad (18e)$$

In the problem (P2.1), the function (18) and constraints (18a)-(18d) are all convex except constraint (18e). This non-convex expression can be handled by applying the SCA algorithm, which replaces the non-convex function with a convex function in continuous iterations until the object value is below the threshold value [26]. For the right-hand-side (RHS) of (18e), the global concave lower bound can be given under the local point $\{\tilde{q}_n^{(l)}\}$ at the $l-$th iteration as follow

$$\log_2\left(1 + \frac{\gamma_0}{\left(H^2 + \|\tilde{q}_n - w_n\|^2\right)^{\alpha}}\right) \ge R_n^{(l)}(\tilde{q}_n), \quad (19)$$

Then, use the lower bound $R_n^{(l)}$ to replace the RHS of (18e). There is a new problem (P2.2):

$$P2.2: \min_{\{\tilde{q}_n, D_t, \eta_n\}} E_0^* D_{tot} + \sum_{n=1}^{N} \frac{(P_h + P_c) Q_n}{B\eta_n} \quad (20)$$

$$s.t. \sum_{n=1}^{N-1} \|\tilde{q}_{n+1} - \tilde{q}_n\|^2 + \|\tilde{q}_1 - \tilde{q}_0\|^2 + \|\tilde{q}_N - \tilde{q}_0\|^2 \le D_{tot}, \quad (20a)$$

$$\eta_n \ge 0, \quad (20b)$$

$$0 \le \tilde{q}_n \cdot x \le L, n = \{1, \ldots, N\}, \quad (20c)$$

$$0 \le \tilde{q}_n \cdot y \le L, n = \{1, \ldots, N\}, \quad (20d)$$

$$\eta_n \le R_n^{(l)}, An. \quad (20e)$$

Problem (P2.2) turns out to be convex, and it is solved by applying the toolbox CVX. And the next step is to keep updating $\tilde{q}_n^{(l)}$ until the object value converges below the threshold. This work summarizes this SCA-based algorithm in algorithm 1. According to [27], the results will finally converge to the Karush-Kuhn-Tucker (KKT) conditions, and the optimal trajectory is obtained under the hovering case as the benchmark.

$R_n^{(l)}(\tilde{q}_n) = \log_2\left(1 + \frac{\gamma_0}{\|\tilde{q}_n^{(l)} - w_n\|^{\alpha}}\right) - \beta_n\left(\|\tilde{q}_n - w_n\|^2 - \|\tilde{q}_n^{(l)} - w_n\|^2\right)$, $\beta_n = \frac{(\log_2 e)\gamma_0 \alpha}{\|\tilde{q}_n^{(l)} - w_n\|^{\alpha}\left(H^2 + \|\tilde{q}_n^{(l)} - w_n\|^2\right)}$

Table 1. Iteration process for P2

1. **Initialize**: set the initial hover location $\tilde{q}_n^{(l)}$, where $l = 0$.

2. **Repeat**:

3. Deal with the convex problem P2.2 and obtain the following optimal variables D_{tot}^*, $\tilde{q}_n^*$, η_n^*.

4. Change the local point as $\tilde{q}_n^{(l+1)} = \tilde{q}_n^*$, An.

5. Change $l = l + 1$.

6. **Until** the object value of P2.2 converges below the threshold ϵ.

3.2. General Solution to (P1)

This section considers the intuitively more general fly-over case where the UAV is flying while communicating with the ground node. The original problem (P 1) involves infinite variables as it is a continuous optimization problem. The other difficulty of solving the problem (P 1) is the non-convexity of the UAV total energy consumption function and required communication throughput constraints.

To tackle the problem (P 1), this paper first introduces the path discretization method to the convert problem (P 1) into a discrete optimization problem. Then, similar to the solution to the problem (P2) in the previous discussion, the slack variables and SCA algorithm are proposed to solve the discrete optimization problem.

3.2.1. Path discretization

The problem (P 1) is a continuous optimization problem, meaning the optimized variables are infinite. The basic idea is discretizing the variables q(t) and λn(t) in order to reformulate (P 1) as a discrete optimization problem. This work introduces the path discretization method, which splits the UAV path into M line segments and yields M + 1 waypoints. Thus, the continuous optimization problem can be converted into a discrete optimization problem.

Specifically, the UAV trajectory variable q(t) is combined with the UAV path and the time dimension. On the one hand, the new variable $\{q_{m1}^{M}+1$ is defined by discretizing the UAV flight path, which is the UAV horizontal coordinates in the flying process. As the need of a closed trajectory, q1 = q0, qM+1 = q0 should be satisfied. Furthermore, it is assumed that the UAV velocity and the distance to each GN are unchanged in each segment qm. Therefore, the new constraints should be defined as follow

$$\|q_{m+1} - q_m\| \le \Delta_{max}, Am, \quad (21)$$

where Δmax is a predetermined value that should be much smaller than the UAV flying altitude to satisfy the assumption. In this case, M should also be chosen efficiently large so that the length of each segment is much less than the total flying distance.

On the other hand, this work denotes Tm as the duration of the line segment m, and this equation to denote the total completion time Tt can be shown as

$$T_t = \sum_{m=1}^{M} T_m. \quad (22)$$

Therefore, the trajectory variable q(t) can be described by variable qm and Tm individually. Then, the velocity of the UAV in segment m can be expressed as

$$V_m = \frac{q_{m+1} - q_m}{T_m}, Am \in \{1, \ldots, M\}, \quad (23)$$

$$\|V_m\| = \frac{\|q_{m+1} - q_m\|}{T_m}, Am \in \{1, \ldots, M\}. \quad (24)$$

The distance between the path segment qm and each GN n can be expressed as $d_{mn} = H^2 + \|q_m - w_n\|^2$, An. Then, the discrete form of the UAV achievable rate can be given by

$$R_{mn} = B \log_2\left(1 + \frac{\gamma_0}{H^2 + \|q_m - w_n\|^2)^{\alpha}}\right). \quad (25)$$

According to the TDMA protocol, the variable $\tau_{mn} \ge 0$ is defined to denote the allocation time for communication in segment m with GN n. In this case, this study imposes constraints $\sum_{n=1}^{N} \tau_{mn} \le T_m$, Am. As a result, the overall transmission rate for GN n can be formed as

$$\bar{R}_n(\{q_m\}, \{\tau_{mn}\}) = B \sum_{m=1}^{M} \tau_{mn} \log_2\left(1 + \frac{\gamma_0}{(H^2 + \|q_m - w_n\|^2)^{\alpha}}\right). \quad (26)$$

For the UAV total energy consumption, the discrete form can be shown as

$$E(\{T_m\}, \{q_m\}, \{\tau_{mn}\}) = \sum_{m=1}^{M} \tau_{mn} P_t \left(\frac{\Delta_m}{T_m}\right) + P_c \sum_{m=1}^{M} \sum_{n=1}^{N} \tau_{mn}$$

$$= P_0 \sum_{m=1}^{M} \left(T_m + \frac{3\Delta_m^2}{T_m}\right) + P_i \sum_{m=1}^{M} \left(T_m^4 + \frac{\Delta_m^4}{T_m^4} - \frac{\Delta_m^2}{T_m^2}\right)^2 + \frac{1}{2} d_0 \rho S A \sum_{m=1}^{M} \frac{\Delta_m^3}{T_m^2} + P_c \sum_{m=1}^{M} \sum_{n=1}^{N} \tau_{mn}, \quad (27)$$

where $\Delta_m \triangleq \|q_{m+1} - q_m\|$, $m \in \{1, \ldots, M\}$ is the length of m − th line segment.

In summary of all the discussions above, the problem (P 1) can be converted into the discrete form (P3) as,

$$\text{P3}: \min_{\{T_m\}, \{q_m\}, \{\tau_{mn}\}} E(\{T_m\}, \{q_m\}, \{\tau_{mn}\}) \quad (28)$$

s.t. 分节符(连续)

$$B \sum_{m=1}^{M} \tau_{mn} \log_2\left(1 + \frac{\gamma_0}{\left(H^2 + \|q_m - w_n\|^2\right)^{\alpha}}\right) \geq Q_n, An, \quad (28a)$$

$$\|q_{m+1} - q_m\| \leq \min\{\Delta_{max}, T_m V_{max}\}, m \in \{1, \ldots, M\}, \quad (28b)$$

$$q_1 = q_0, q_{M+1} = q_0, \quad (28c)$$

$$0 \leq q_{m,x} \leq L, m = \{1, \ldots, M\}, \quad (28d)$$

$$0 \leq q_{m,y} \leq L, m = \{1, \ldots, M\}, \quad (28e)$$

$$\sum_{n=1}^{N} \tau_{mn} \leq T_m, Am, \quad (28f)$$

$$\tau_{mn} \geq 0, Am, n, \quad (28g)$$

where the constraint (28b) refers to the UAV's maximum speed and the maximum segment length, which this paper mentioned before.

In the end, the new problem (P3) is in the discrete form, which is more tractable. However, (P3) is still a non- convex problem because of the non-convexity of the discrete energy consumption function and the throughput requirement constraint. Similar to section 3. 1, the slack variables and the SCA algorithm can be used.

3.2.2. UAV energy consumption minimization in (P3)

As mentioned before, the object function of the problem (P3) and the constraint (28a) are both non-convex. The UAV's energy consumption function can prove that only the second term is non-convex through the perspective

operation [28]. Therefore, this research introduces the slack variable $y_m \geq 0$ to denote the term $\hat{T}m(4) + - .$ Then the following relationship is given by

$$y_m^2 = \sqrt{T_m^4 + \frac{\Delta_m^4}{4v_0^4}} - \frac{\Delta_m^2}{2v_0^2}, Am, \quad (29)$$

which is also

$$\frac{T_m^4}{y_m^2} = y_m^2 + \frac{\Delta_m^2}{v_0^2}, Am. \quad (30)$$

Then, the second term of the UAV energy consumption can be expressed as the convex linear form $P0 \sum_{m=1}^{M} ym$ by imposing the additional constraints as

$$\frac{T_m^4}{y_m^2} \leq y_m^2 + \frac{\|q_{m+1} - q_m\|^2}{v_0^2}, Am. \quad (31)$$

The RHS of (31) should be transferred to the concave or affine form by deriving the first-order Taylor expansion as the global lower bound of it as

$$y_m^2 + \frac{\|q_{m+1} - q_m\|^2}{v_0^2} \geq y_m^{(l)2} + 2y_m^{(l)}(y_m - y_m^{(l)}) - \frac{\|q_m^{(l)} - q_m\|^2}{v_0^2} + \frac{2}{v_0^2}(q_{m+1}^{(l)} - q_m^{(l)})^T (q_{m+1} - q_m), \quad (32)$$

where $y_m^{(l)}$ and $q_m^{(l)}$ are both the local point at l − th iteration.

As for the non-convex constraint of the communication throughput requirement, this work also uses the slack variable $\{A_{mn}\} \geq 0$ to replace the original expression as

$$A^2 = \log_2\left(1 + \frac{\gamma_0}{\left(H^2 + \|q_m - w_n\|^2\right)^{\alpha}}\right), \quad (33)$$

Then, constraint (28a) is converted into $B\sum_{m=1}^{M} A_{mn}^2 \geq Q_n, An.$ Also, there is a new constraint as

$$\frac{A_{mn}^2}{\tau_{mn}} \leq \log_2\left(1 + \frac{\gamma_0}{\left(H^2 + \|q_m - w_n\|^2\right)^{\alpha}}\right), Am, n. \quad (34)$$

Firstly, for the constraint $B\sum_{m=1}^{M} A_{mn}^2 \geq Q_n, An$, the left-hand-side (LHS) is a convex function while it should be converted into the concave or affine form. This paper thus uses the first-order Taylor expansion as the global lower bound of A_{mn}^2, and the inequality can be shown as

$$A_{mn}^2 \geq A_{mn}^{(l)2} + 2A_{mn}^{(l)}(A_{mn} - A_{mn}^{(l)}), \quad (35)$$

where $A_{mn}^{(l)}$ denotes the value of A_{mn} at iteration l.

Then, by applying the same technique as the operation to (19), the global lower bond of RHS of (34) is expressed as,

$$\log_2\left(1 + \frac{\gamma_0}{\left(H^2 + \|q_m - w_n\|^2\right)^{\alpha}}\right) \geq R_{mn}^{(l)}(q_m)^2, \quad (36)$$

As a result, the new problem (P3.1), which introduces the slack variables and apply SCA techniques, can be given by,

$$\text{P3.1}: \min_{\{y_m, q_m, \tau_{mn}, v_m, A_{mn}\}} P_0 \sum_{m=1}^{M}\left(T_m + \frac{3\Delta_m^2}{U_{tip}^2 T_m}\right) + P_1 \sum_{m=1}^{M} y_m + \frac{1}{2} d_0 \rho s A \sum_{m=1}^{M} \frac{\Delta_m^3}{T_m^2} + P_c \sum_{m=1}^{M}\sum_{n=1}^{N} \tau_{mn} \quad (37)$$

s.t.

$$B\sum_{m=1}^{M} A_{mn}^{(l)2} + 2A_{mn}^{(l)}(A_{mn} - A_{mn}^{(l)}) \geq Q_n, An, \quad (37a)$$

$$\frac{T_m^4}{y_m^2} \leq y_m^{(l)2} + 2y_m^{(l)}(y_m - y_m^{(l)}) - \frac{\|q_{m+1}^{(l)} - q_m^{(l)}\|^2}{v_0^2} + \frac{2}{v_0^2}(q_{m+1}^{(l)} - q_m^{(l)})^T (q_{m+1} - q_m), Am, \quad (37b)$$

$$\frac{A_{mn}^2}{\tau_{mn}} \leq R_{mn}^{(l)}(q_m), Am, n, \quad (37c)$$

$$y_m \geq 0, Am, \quad (37d)$$

$$A_{mn} \geq 0, Am, n, \quad (37e)$$

$$(28b) - (28g). \quad (37f)$$

Problem (P3.1) can also be handled by using the CVX toolbox. Then, this work successively updates the local points $q_m^{(l)}$, $T_m^{(l)}$ and $\tau_{mn}^{(l)}$ by solving the problem (P3.2). The iteration is stopped when the object value converges to a certain threshold. This SCA process is firstly doing the initialization, which obtains the feasible $q_m^{(0)}$, $T_m^{(0)}$ and $\tau_{mn}^{(0)}$ to (P3). The next step is starting the iteration, and in the loop, $y_m^{(l)}$ and $A_{mn}^{(l)}$ based on (32) and (34) are calculated. Then, solve (P3.2) and have the optimal $\{q_m^*\}$, $\{T_m^*\}$ and $\{\tau_{mn}^*\}$ as the updating local points. The following work is to repeat the loop until reaching the threshold. The above process is concluded as Algorithm 2. Finally, the obtained trajectory is called the fly-over trajectory.

In this way, the optimal UAV flight trajectory, optimal UAV communication allocation time, and minimum UAV energy consumption are obtained.

$$R_{mn}^{(l)}(q_m) = \log_2\left(1 + \frac{\gamma_0}{\left(H^2 + \|q_m^{(l)} - w_n\|^2\right)^{\alpha}}\right) - \beta_{mn}\left(\|q_m - w_n\|^2 - \|q_m^{(l)} - w_n\|^2\right),$$

$$\beta_{mn} = \frac{\log_2(e)\gamma_0\alpha}{\left(H^2 + \|q_m^{(l)} - w_n\|^2\right)\left(H^2 + \|q_m - w_n\|^2\right)^{\alpha+1}}.$$

Table 2. Iteration process for P

1. **Initialize**: set the initial feasible $\{q_m^{(0)}\}$, $\{T_m^{(0)}\}$ and $\{\tau_{mn}^{(0)}\}$ to (P3.1), where $l = 0$.
2. **Repeat**:
3. Calculate local points $y_m^{(l)}$ and $A_{mn}^{(l)}$ individually.
4. Solve the convex problem P3.1 and obtain the following optimal variables $\{q_m^*\}$, $\{T_m^*\}$ and $\{\tau_{mn}^*\}$.
5. Change the local points as $q_m^{(l+1)} = q_m^*$, $T_m^{(l+1)} = T_m^*$ and $\tau_{mn}^{(l+1)} = \tau_{mn}^*$.
6. Change $l = l + 1$.
7. **Until** the object value of P3.1 converges below the threshold ϵ.

4. Numerical Results

4.1. Parameters Setting

This section describes the parameters set in the system model and the numerical results ofthe proposed problem. In the system model, this work uses the rotary-wing UAV as the FBS, so the UAV-related attributes for the UAV propulsion power are set as shown in table 1. The communication power consumption of the UAV is set to be a constant as Pc = 5W [29]. Then, the maximum UAV velocity is required that Vma 北 = 30m/s and the fixed UAV flying altitude H is 100m. This is by Federal Aviation Administration (FAA) regulations that small UAVs cannot fly above 400 feet in altitude [30]. For the communication system, this work defines the communication bandwidth as B = 1MHz, and the reference SNR is set to be γ0 = 52.5dB with transmit power P = 20dBm. For the model scenario, the length of the hypothetical square map is L = 1200m. The location of the ground base station is at the center of the virtual map at q0 = [600m, 600m] T, and this research uses q0 as the initial and final location of the UAV. The number of GN is set to N = 10. Additionally, the required communication throughput Qn for GN n is assumed to be identical among all GNs where Qn = $\bar{Q}$. Furthermore, it is defined that Δmax = 30 m. For the Algorithm 1, the initial hover locations $\tilde{q}_n^{(0)}$ is set to be the GN's locations wn which is $\tilde{q}_n^{(0)}$ = wn, Am. For the Algorithm 2, this paper divides the UAV trajectory q(t) into M line segments where

M = 250. The initial local point $\{q_m^{(0)}\}$ of the UAV discrete path is set as the obtained optimal UAV path by Algorithm

1. For the other two local points, which are initial duration

time $\{T_m^{(0)}\}$ and initial communicate allocation time $\{\tau_{mn}^{(0)}\}$ individually, this paper has $T_m^{(0)} = \bar{T}$, Am, and $\tau_{mn}^{(0)} = \frac{\bar{T}}{N}$, Am, n. $\bar{T}$ is set as the minimum value that makes all the constraints feasible in (P3). Then, the work uses the SCA-based Algorithm 2 to obtain the optimal trajectory in the case that the UAV flies while communicating with the GN. These two schemes will be compared later at different required communication throughputs.

Table 3. The rotary-wing UAV attribute

Notation	Physical meaning	Simulation value
δ	Profile drag coefficient	0.012
ρ	Air density	1.225
W	Aircraft weight in Newton	20
d_0	Fuselage drag ratio	0.6
R	Rotor radius	0.4
Ω	Blade angular velocity	300
k	Incremental correction factor	0.1
U_{tip}	Tip speed of rotor blade	120
A	Rotor disc area	0.503
s	Rotor solidity	0.05
v_0	Mean rotor induced velocity in hover	4.03

4.2. Results and Analyses

The simulation results first propose four different required communication throughputs $\bar{Q}$ to the formulated optimization problem (P 1) and compare the difference between the benchmark solution in (P2) and the more general fly-over trajectory in (P3) as shown in Fig. 3.

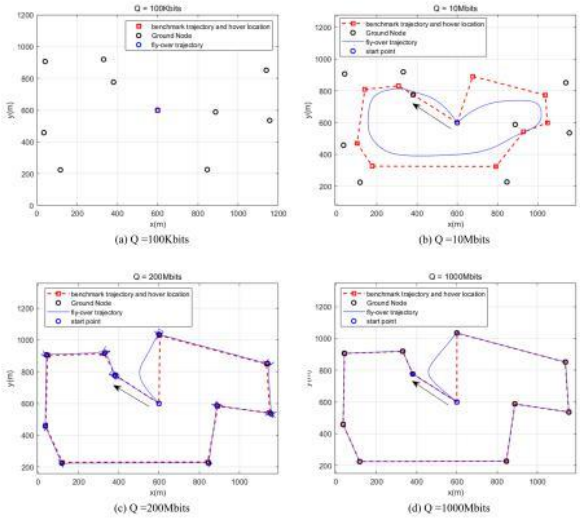

Figure 2. Optimized UAV trajectories with four different communication demands

When the required communication throughput is extremely low, where $\bar{Q}$ = 100Kbits, the UAV hovers at the de- parture point and communicates with each GN regardless of the design of the UAV for communication. It is notable that as the UAV gets closer to the GN, the shorter the distance of the communication link between them, which will consume less energy generated by hovering and communication. However, this will also make the UAV fly longer distances, thus increasing the propulsion energy consumed by the UAV. Therefore, when the GN has low demand for communication, the time required for the UAV serving to each GN is much less than the time required to fly to each GN. In this case, there is no need for the UAV to fly toward the GNs based on the fact that the hover power and communication power are much less than the UAV propulsion power with a short period of serving time. Similarly, when the demand for GNs is hugely high, where $\bar{Q}$ = 1000Mbits, the two trajectories under different communication designs are quite identical. For the fly-hover-communicate scheme of the UAV, it is shown that the UAV should hover precisely on the location of each GN above. For the general fly-over case, the trajectory is the same as the benchmark except for the path where the UAV returns to the ground base station. Moreover, it is notable that from Fig. 4(c), the UAV speed of the fly-over design is nearly equal to zero for a period when the UAV reaches each GN. This means that when the required communication throughput is exceptionally high, the optimal solution to the least energy consumption is that the UAV still needs to hover on the top of the GN to provide service but at a shorter flying distance and a little lower flying speed. It is expected because in this case, the time required for communication is very long, so reducing the communication time is more effective in saving the total energy consumption than reducing the UAV flight distance.

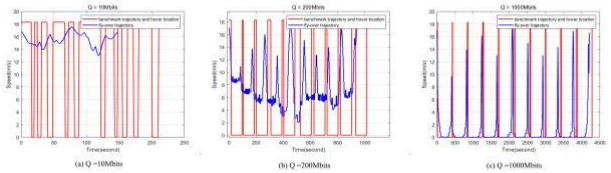

Figure 3. Optimized UAV speed for different trajectories

On the other hand, in terms of moderate required communication throughput where $\bar{Q}$ = 10Mbits and $\bar{Q}$ = 200Mbits, the optimized hover locations are generally different from the GN locations. From Fig. 3(b) ($\bar{Q}$ = 10Mbits), it is notable that most of the optimized hover locations are closer to the centrally located ground base station than the GN locations, which means the UAV flying distance is reduced. For the fly-over scheme, the distance of optimal UAV trajectory is even shorter. In this case, the UAV keeps flying at a lower speed throughout the process until it returns to the ground base station (shown in Fig. 4(a)). Alternatively, when the required throughput increases to $\bar{Q}$ = 200Mbits, the optimized hover locations get much closer to the GN locations, and the hover time is correspondingly increasing. In contrast, for the fly-over scheme, when the UAV approaches the GN, the figure shows that the UAV does not hover above the GN but will maintain a constant speed to fly around the GN. This seems to be contrary to the previous analysis because the UAV is flying around the GN, which would lead to a longer link distance and flight distance. However, this is reasonable because keeping hover status is not the ideal energy-conserving state for rotary-wing UAVs [20]. Therefore, even if the UAV is exactly on top of the GN, it should keep flying in order to both minimize the power consumption and the communication time. In other words, this also shows that the time required for UAV communication and the flight distance have similar effects on the total energy consumption at $\bar{Q}$ = 200Mbits.

In the following, the energy consumption with three UAV trajectory designs under the varying required throughputs is compared as shown in Fig. 5. The blue and red lines are two schemes this work discussed before, and the green line

denotes the trajectory that the UAV is required to hover above GNs. From Fig. 5, it is shown that the three trajectories are relatively similar when $\bar{Q}$ is particularly small. As $\bar{Q}$ increases, the trajectory with the fly-over scheme always saves

more energy. In the contrast, the benchmark trajectory under the fly-hover-communicate protocol keeps the same as that with hover on the top of GNs after $\bar{Q}$ is larger than 100Mbits.

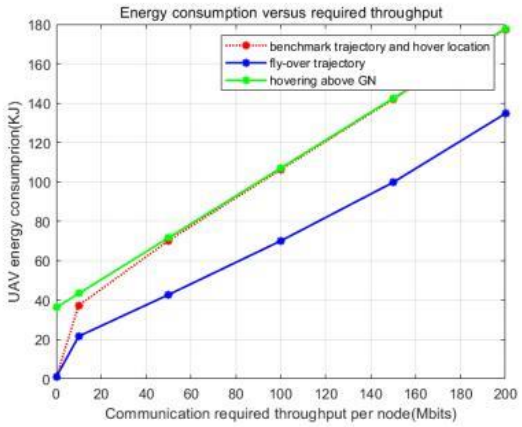

Figure 4. Energy consumption versus required throughput

In terms ofthe difference between the benchmark result and the fly-over result, Fig. 6 gives the energy-saving amount and rate that the fly-over trajectory design can make with the increasing required throughput. When $\bar{Q}$ = 200Mbits, the proposed fly-over design saves the most amount of energy because the required communication time and the flight distance have an equal influence on the energy consumption under this throughput constraint. Then, under the SCA-based algorithm, the most optimal status between the two factors can be balanced. However, the saving efficiency is highest when $\bar{Q}$ = 10Mbits from the saving rate curve. This is because although the energy-saving amount of the fly-over scheme is not the highest at $\bar{Q}$ = 10Mbits, the total energy required at this point is lower, resulting in a higher savings rate. Also, these two mountain-shaped curves show that the energy-saving performance of the fly-over scheme decreases when $\bar{Q}$ is particularly smaller and larger. More specifically, the UAV still needs to be in static status while serving the GN, whether demand is too high or low. In general, the fly-over scheme is a more energy-efficient trajectory design compared to the benchmark. In the extreme case, the performance of the two schemes converges to the same in terms of total energy consumption

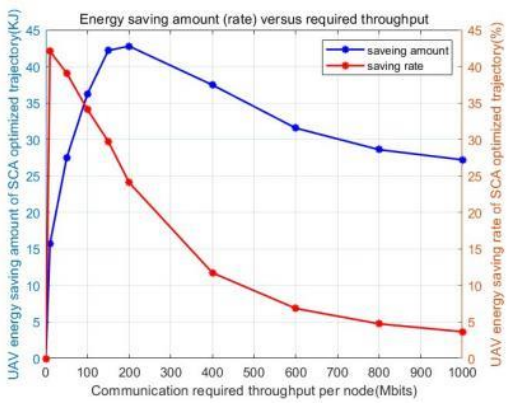

Figure 5. Energy-saving amount (rate) versus required throughput

5. Conclusion

This project investigates the design of closed, energy-efficient flight trajectories during UAV-to-ground communica- tions. This work uses a rotary-wing UAV as the object of study and constructs an optimization problem with its energy consumption model as the objective function. Two UAV flight modes are considered, one is to fly to a particular position and hover to communicate with GNs, called the fly-hover-communicate scheme as the benchmark, and the other is to fly while communicating with GNs, named the fly-over scheme. The results show that the second trajectory design scheme is usually more energy efficient than the benchmark under specific communication throughput requirements. However, the performance for energy saving tends to be the same when the user demand is very low or very high. Therefore, a reference can be given for designing UAV trajectories in different situations. For instance, when the data transmission rate required

by the regional node is not high, the UAV can just hover at the original location to provide services to the surrounding user community instead of letting it fly. When the demand for regional nodes increases, for example, in a post-disaster recon- struction scenario, the best trajectory can be designed based on the fly-over scheme. Furthermore, with the development of the Internet of Things, the user demand for communication is extremely high when a simpler fly-hover-communicate scheme can be used and can be combined with a gripper installed on the hover point [31] to reduce the energy consumed by the drone hovering.

Acknowledgements

I would like to thank Dr.Vasilis Friderikos (King's College London) for the research supervision and discussions.

References

[1] Zeng Y, Zhang R, Lim T J. Wireless communications with unmanned aerial vehicles: Opportunities and chal-lenges[J]. IEEE Communications magazine, 2016, 54(5): 36-42.

[2] Chakareski J, Naqvi S, Mastronarde N, et al. An energy efficient framework for UAV-assisted millimeter wave 5G heterogeneous cellular networks[J]. IEEE Transactions on Green Communications and Networking, 2019, 3(1): 37-44.

[3] Namuduri K, Wan Y, Gomathisankaran M. Mobile ad hoc networks in the sky: State ofthe art, opportunities, and challenges[C]//Proceedings of the second ACM MobiHoc workshop on Airborne networks and communications. 2013: 25-28.

[4] Mozaffari M, Saad W, Bennis M, et al. A tutorial on UAVs for wireless networks: Applications, challenges, and open problems[J]. IEEE communications surveys & tutorials, 2019, 21(3): 2334-2360.

[5] Wang J, Jiang C, Han Z, et al. Taking drones to the next level: Cooperative distributed unmanned-aerial-vehicular networks for small and mini drones[J]. Ieee vehIcular technology magazIne, 2017, 12(3): 73-82.

[6] Wang J, Jiang C, Wei Z, et al. Joint UAV hovering altitude and power control for space-air-ground IoT networks[J]. IEEE Internet ofThings Journal, 2018, 6(2): 1741-1753.

[7] Huo Y, Dong X, Lu T, et al. Distributed and multi-layer UAV network for the next-generation wireless communi-cation[J]. arXiv preprint arXiv:1805.01534, 2018.

[8] Al-Hourani A, Kandeepan S, Lardner S. Optimal LAP altitude for maximum coverage[J]. IEEE Wireless Commu-nications Letters, 2014, 3(6): 569-572.

[9] Li B, Chen C, Zhang R, et al. The energy-efficient UAV-based BS coverage in air-to-ground communica-tions[C]//2018 IEEE 10th Sensor Array and Multichannel Signal Processing Workshop (SAM). IEEE, 2018: 578- 581.

[10] Mozaffari M, Saad W, Bennis M, et al. Drone small cells in the clouds: Design, deployment and performance analysis[C]//2015 IEEE global communications conference (GLOBECOM). IEEE, 2015: 1-6.

[11] Wu Q, Liu L, Zhang R. Fundamental trade-offs in communication and trajectory design for UAV-enabled wireless network[J]. IEEE Wireless Communications, 2019, 26(1): 36-44.

[12] Zeng Y, Zhang R, Lim T J. Throughput maximization for UAV-enabled mobile relaying systems[J]. IEEE Trans-actions on communications, 2016, 64(12): 4983-4996.

[13] Wu Q, Zeng Y, Zhang R. Joint trajectory and communication design for multi-UAV enabled wireless networks[J]. IEEE Transactions on Wireless Communications, 2018, 17(3): 2109-2121.

[14] Xu J, Zeng Y, Zhang R. UAV □ Enabled Wireless Power Transfer[J]. UAV Communications for 5G and Beyond,2020: 399-416.

[15] Zhang G, Wu Q, Cui M, et al. Securing UAV communications via joint trajectory and power control[J]. IEEE Transactions on Wireless Communications, 2019, 18(2): 1376-1389.

[16] Lee W, Jeon Y, Kim T, et al. Deep Reinforcement Learning for UAV Trajectory Design Considering Mobile Ground Users[J]. Sensors, 2021, 21(24): 8239.

[17] Zeng Y, Zhang R. Energy-efficient UAV communication with trajectory optimization[J]. IEEE Transactions on Wireless Communications, 2017, 16(6): 3747-3760

[18] Yang D, Wu Q, Zeng Y, et al. Energy tradeoff in ground-to-UAV communication via trajectory design[J]. IEEE Transactions on Vehicular Technology, 2018, 67(7): 6721-6726.

[19] Hua M, Wang Y, Zhang Z, et al. Power-efficient communication in UAV-aided wireless sensor networks[J]. IEEE Communications Letters, 2018, 22(6): 1264- 1267.

[20] Zeng Y, Xu J, Zhang R. Energy minimization for wireless communication with rotary-wing UAV[J]. IEEE Trans-actions on Wireless Communications, 2019, 18(4): 2329-2345.

[21] Lu R R, Ma Y, Lin S H, et al. Energy-efficient trajectory optimization for UAV-based hybrid FSO/RF communica-tions with buffer constraints[J]. Entropy, 2021, 23(12): 1596.

[22] Salehi S, Bokani A, Hassan J, et al. Aetd: An application-aware, energy-efficient trajectory design for flying base stations[C]//2019 IEEE 14th Malaysia International Conference on Communication (MICC). IEEE, 2019: 19-24.

[23] Salehi S, Hassan J, Bokani A, et al. A QoS-aware, energy-efficient trajectory optimization for UAV base stations us-ing Q-learning[C]//2020 19th ACM/IEEE International Conference on Information Processing in Sensor Networks (IPSN). IEEE, 2020: 329-330.

[24] Lan T, Qin D, Sun G. Joint Optimization on Trajectory, Cache Placement, and Transmission Power for Minimum Mission Time in UAV-Aided Wireless Networks[J]. ISPRS International Journal of Geo-Information, 2021, 10(7): 426.

[25] Jing X, Sun J, Masouros C. Energy aware trajectory optimization for aerial base stations[J]. IEEE Transactions on Communications, 2021, 69(5): 3352-3366.

[26] Razaviyayn M. Successive convex approximation: Analysis and applications[D]. University of Minnesota, 2014.

[27] Zappone A, Björnson E, Sanguinetti L, et al. Globally optimal energy-efficient power control and receiver design in wireless networks[J]. IEEE Transactions on Signal Processing, 2017, 65(11): 2844-2859.

[28] Boyd S, Boyd S P, Vandenberghe L. Convex optimization[M]. Cambridge university press, 2004.

[29] Arnold O, Richter F, Fettweis G, et al. Power consumption modeling of different base station types in heterogeneous cellular networks[C]//2010 Future Network & Mobile Summit. IEEE, 2010: 1-8.

[30] FAA. Summary of Small Unmanned Aircraft Rule. Accessed: Feb. 18, 2019. [Online]. Available: https : // www.faa.gov / uas / media/Part107Summary.pdf

[31] V. Friderikos, ”Airborne Urban Microcells with Grasping End Effectors: A Game Changer for 6G Networks?,” 2021 IEEE International Mediterranean Conference on Communications and Networking (MeditCom), 2021, pp. 336-341, doi: 10. 1109/MeditCom49071.2021.9647696.